Available online at www.sciencedirect.com
ScienceDirect
Surface Science 601 (2007) 352–361
SURFACE SCIENCE
www.elsevier.com/locate/susc

Surface structure of sphalerite studied by medium energy ion scattering and XPS

S.L. Harmer [a,*], L.V. Goncharova [b], R. Kolarova [c,1], W.N. Lennard [c], M.A. Muñoz-Márquez [d,2], I.V. Mitchell [c], H.W. Nesbitt [a]

[a] Department of Earth Science, University of Western Ontario, London, Ontario, Canada N6A 5B7
[b] Department of Physics and Astronomy, Rutgers University, 136 Frelinghuysen Road, Piscataway, NJ 08854-8019, USA
[c] Department of Physics and Astronomy, University of Western Ontario, London, Ontario, Canada N6A 3K7
[d] Department of Physics, University of Warwick, Coventry CV4 7AL, UK

Received 14 July 2006; accepted for publication 3 October 2006
Available online 24 October 2006

Abstract

The reactivity of high-Fe containing sphalerite ($Zn_{1-x}Fe_xS$), the major source of Zn, is of great interest for industrial applications. Since the initial reactivity depends on the physical and chemical properties of the surface, it is important to understand the structure of cleaved and fractured surfaces. $Zn_{1-x}Fe_xS$ zincblende (1 1 0) oriented samples cleaved in air and in vacuum were studied with medium energy ion scattering (MEIS) in order to study surface relaxation and reconstruction associated with the possible formation of S dimers. The experimental results are presented together with ion scattering Monte Carlo simulations that have been performed using the different models of the surface structure. The MEIS blocking patterns are different for the air- and vacuum-cleaved specimens. Models for the air-cleaved samples found S atoms in the first layer that are relaxed outwards by 0.08 Å and Zn(Fe) atoms relaxed inwards by 0.51 Å, with some lateral translation of both species. Results for the vacuum-cleaved sample indicate S atoms have been displaced laterally by 0.5 Å at the surface. X-ray photoelectron spectroscopic (XPS) measurements provide evidence for a high binding energy species indicative of S–S bonds in the near-surface region that are consistent with the ion scattering structural data for both cleaving protocols.

Keywords: X-ray photoelectron spectroscopy; Medium energy ion scattering; Surface structure; Sphalerite; ZnS; Photoelectron emission; Wide bandgap semiconductor

1. Introduction

Naturally occurring Fe-containing sphalerite $Zn_xFe_{1-x}S$ is the world's primary source of Zn. A knowledge of the surface composition and structure for a number of metal sulfides is of critical importance in the control of mineral surface reactivity, for mineral separation by flotation and in sulfide mineral leaching for metal recovery or control of environmental pollution [1,2]. The mineral industry generally crushes sulfide ores during processing, so that the surfaces of all ores separated by flotation represent varied fracture surfaces. Pure ZnS is a large bandgap ($E_g = 3.7$ eV) II–VI semiconductor – a material for which doping with Fe causes a decrease in the band gap with increasing Fe content [3].

Both sphalerite (β-ZnS), with the zincblende crystal structure (lattice constant = 5.4093 Å), and wurtzite (α-ZnS) forms of ZnS undergo considerable relaxation of surface atoms. Sphalerite has been examined using low energy

* Corresponding author. Present address: Ian Wark Research Institute-AMSRI, University of South Australia, Mawson Lakes Campus, Mawson Lakes, SA 5095, Australia.
E-mail address: sarah.harmer@unisa.edu.au (S.L. Harmer).
[1] Present address: Department of Atomic Physics and Surface Science, Institute of Experimental Physics, Johannes Kepler Universität, Altenbergerstrasse 69, A-4040, Linz, Austria.
[2] Present address: Instituto de Ciencia de Materiales de Sevilla, Américo Vespucio s/n, 41092 Seville, Spain.

0039-6028/$ - see front matter © 2006 Elsevier B.V. All rights reserved.
doi:10.1016/j.susc.2006.10.001

electron diffraction (LEED), particularly the {1 1 0} perfect cleavage surface [4–7]. We note that, in general, investigations of these insulating materials using an electron beam (or *any* charged particle) have proved challenging due to charging phenomena. These studies have revealed a perpendicular movement of the first layer Zn atoms (cations) *toward* the bulk by 0.51 Å, with first layer S atoms (anions) moving *outward* by 0.08 Å, resulting in the so-called 'puckering' of the upper layer of S atoms above the corresponding Zn atom layer. There is evidence of some lateral surface layer reconstruction. Theoretical density functional calculations [8] have successfully modeled this structure. Additionally, Vaughan et al. [2] have noted that Zn atoms in the second layer move inwards by 0.14 Å. Note that the early LEED studies were performed on atomically clean surfaces that were prepared via sputtering and long time (~4 h) annealing at 650 °C in ultra-high vacuum (UHV) – a situation that is quite different both from the present studies and from those relevant for the mineral recovery process. It is possible for a lengthy annealing process to induce surface structural modifications.

Numerous questions remain concerning differences between the 'clean' surface of a mineral sulfide (in vacuum or in an inert environment) and the bulk. The surface reactivity in air or aqueous solution is also unresolved. The composition and structure of the sphalerite surface have been investigated previously via Rutherford backscattering spectrometry (RBS) [9,10] (but without monolayer resolution), XPS [1,9,11–13], secondary ion mass spectrometry (ToF-SIMS) [1,12,13] and, as mentioned previously, LEED [4–7]. The formation of sulfur polymers is known to increase the hydrophobicity of the surface layers and it is known that the reactivity of $Zn_xFe_{1-x}S$ increases with increasing Fe content [1].

In this work, a first attempt to study the (1 1 0) sphalerite surface has been made using the MEIS technique with an aim to verify high resolution XPS results that infer surface sulphur dimerization. MEIS is a high resolution variant of RBS wherein elastically scattered projectiles (*i.e.* H and He ions) are energy and angle analyzed by a toroidal electrostatic analyzer (TEA), instead of using a Si charged particle detector as used in conventional RBS. In general, the method lends itself to surface science applications for single crystal specimens (monoelemental or binary alloys) and requires the use of channeling conditions for the incident ions. In such a configuration, the target is oriented such that incident charged particles are parallel to a major (*i.e.* low index) crystallographic direction. The TEA is positioned such that the central angle corresponds to a blocking geometry for the outward scattered ions, *i.e.* those ions emerge parallel to another major crystallographic direction. Thus, the geometrical technique is often described as a 'double alignment' method. Scattered yields are measured over a wide angular range, typically 30°, with a relative energy resolution $\Delta E/E \approx 0.2\%$ in favourable cases. Target species identification and depth distributions are given by the known scattering kinematics, as with conventional RBS. The shadowing and blocking capabilities of MEIS provide a unique means to determine surface structure coupled with layer-by-layer depth profile information. Several reports are available describing the principles of the technique [14–20]. Extensive Monte Carlo computer simulations are required to extract atomic positions from measured yields. Such data are complementary to XPS investigations in that the MEIS measurements are insensitive to chemical bonding and can, in favourable situations, determine atomic positions and *absolute* areal densities directly, including surface relaxations and reconstructions.

2. Experiments

The sphalerite specimens chosen for the present investigations originated in Nacia, Mexico and were of high-Fe content type, *i.e.* $Zn_{1-x}Fe_xS$, where $x \approx 0.25$. The {1 1 0} surfaces are known to be easily cleaved for this material [21]. The surface treatment chosen for the various studies depended on the type of information that was being sought: for the electron probe microanalysis (EPMA), Rutherford backscattering (RBS) and particle-induced X-ray emission (PIXE) measurements where bulk properties are examined, samples were cleaved in air and subsequently loaded into the analysis chamber, thereby precluding any determination of surface structure or composition on an atomic scale. For all the ion beam studies, no deleterious effects caused by sample charging were observed.

In order to ascertain the bulk stoichiometry of the present $Zn_{1-x}Fe_xS$ sphalerite targets, a conventional RBS spectrum corresponding to incident 2.0 MeV $^4He^+$ ions accelerated by a 1.7 MV Tandetron facility was recorded with a Si charged particle detector positioned at a scattering angle of 170°. The sample was continuously rotated around the azimuth with a tilt angle of 2.5° during the data acquisition in order to avoid channeling effects: such a spectrum then corresponds to a 'random' alignment. Additionally, quantitative electron microprobe analysis (EPMA) was performed by wavelength dispersive spectrometry using a JEOL 8900 electron microprobe operated at 20 kV and 20 nA.

For the PIXE measurements, the $Zn_{1-x}Fe_xS$ sample was bombarded with normally incident 1 MeV $^4He^+$ ions produced by the UWO 2.5 Van de Graaff accelerator, with a beam (on target) footprint size of $\sim 0.5 \times 0.5$ mm^2. The S, Fe and Zn K X-ray yields were measured as a function of target tilt angle around the $\langle 1\,1\,0 \rangle$ axial channelling direction in order to determine the position of Fe atoms with regard to Zn atoms in the bulk. Additional K and L X-ray peaks arising from Mn and Cd, respectively, were also recorded. The RBS spectra were acquired simultaneously with a Si charged particle detector positioned at 150°. The PIXE spectra were acquired with a cooled HPGe detector (resolution 135 eV at 5.9 keV) having a 5 mm diameter Be entrance window of thickness 13 μm, positioned at an observation angle of 135° relative to the incident beam direction to minimize the bremsstrahlung X-ray

yield. The detector window was covered by an Al foil of thickness 8.3 μm to attenuate the low energy X-ray flux. The sample was attached with vacuum grease to the sample holder. However, a metallic clip was placed in direct contact with the sample to assure adequate electrical conductivity. (We note that surface structure studies using ionizing radiation can sometimes be plagued by charging problems for this material.)

For the X-ray photoelectron spectroscopy (XPS) studies, a sphalerite sample was held at $T < 200$ K and cleaved in vacuum at 4×10^{-8} torr prior to transfer into the analytical chamber for analysis at 8×10^{-10} torr. Note that elemental surface sulphur is expected to evaporate in vacuum for $T > 200$ K, although elemental sulphur is not expected here [22]. XPS spectra were collected using a Kratos Axis Ultra spectrometer fitted with a monochromatic Al K_α source (1487 eV) operating at 15 kV and 14 mA with a spot size of 300 μm. A charge neutralization system using a novel magnetic lens was employed to replace electrons lost at the sample surface; this system yields much narrower XPS linewidths on non-conducting samples in comparison to other charge neutralization systems [23]. Survey scans were collected using a pass energy of 160 eV and a step size of 0.7 eV to ensure purity of the sample and cleanliness of the fracture. High resolution spectra were collected at 10 eV pass energy using a step size of 0.025 eV. The spectrometer was standardized to Au $4f_{7/2}$ at 84.00 eV and calibrated using Cu $2p_{3/2}$ at 936.6 eV.

For the MEIS measurements, sphalerite samples were cleaved in an enclosed glovebag purged with inert dry Ar (at UWO, $T = 300$ K throughout) and loaded as quickly as possible into a load-lock chamber in an effort to minimize oxidation. It is known that most metal sulfides are relatively reactive and are not stable in oxidizing aqueous solutions (or at the level of the surface monolayer, in air) [2]. Preliminary measurements were made at UWO using 100 keV $^1H^-$ ions produced by a 1.7 MV high current Tandetron accelerator; the Fe and Zn contributions were incompletely resolved with regard to mass for incident proton beams. We note in passing that scattered proton spectra are independent of the charge carried by the incident ^1H ions. To resolve the Fe and Zn species, the MEIS experiments were continued at Rutgers University where a high flux 130.3 keV $^4He^+$ ion beam was available from a HVEE 400 kV ion implanter coupled to a UHV chamber with a base pressure $\sim 2 \times 10^{-10}$ torr. Two sets of measurements were performed using incident $^4He^+$ ions: for one, the sample was cleaved in air prior to insertion into the UHV; for the second, the sample was cleaved in 10^{-8} torr before insertion into the UHV system. However, it is difficult to assert that the sphalerite sample surfaces would not become contaminated for all the MEIS measurements, since the data acquisition occurs over a time period of a few *hours* in order to obtain a complete spectrum and hydrocarbon contamination of the sphalerite mineral surface has been assumed in other works [12]. Even in UHV, and even when moving the beam spot on the target at regular intervals, the sample surface can become contaminated with either water vapour or condensible hydrocarbons. Steele et al. [8] have shown that H_2O adsorption on the sphalerite surface is energetically favourable in two more or less similar configurations. This surface contamination issue will become important in a discussion of the magnitude of the scattered charged particle fraction for incident $^4He^+$ ions that are detected via the MEIS technique. In fact, the MEIS data interpretation in this work would be more controversial in the event that the sphalerite (1 1 0) surface remained atomically clean.

For all MEIS measurements, the samples remained at room temperature. The target holder and detection system used by both MEIS facilities was similar: each setup comprised a three-rotation axis goniometer and elastically scattered ions were analyzed via a TEA fitted with a position sensitive detector (PSD) at the exit position to record both scattering angle and energy. The incident beam fluence was integrated directly from the (positively biased) target. The ions impinged on a target through a set of slits. The final slits had a size of 1 mm in the horizontal direction and 0.25 mm in the vertical direction, where the latter direction corresponds to the dispersion direction for the TEA. Sample alignment to a specific channeling direction, specifically $\langle 1\,1\,0 \rangle$ for the ^4He measurements, was achieved using a Si detector positioned at a backward scattering angle. The TEA was a commercially available HVEE type. The PSD produces two-dimensional intensity maps of the ion intensity over a 1.2% range of pass energy and a scattering angle range (θ) of 24° with a resolution $\Delta E/E \approx 0.2\%$ and $\Delta\theta = 0.15°$ [20]. Full 2D data sets are acquired by taking a series of 'tiles' which span the required energy/angle range and joining them together within a program code to produce a single scattered ion intensity map. While 2D data sets provide a complete picture of the scattering behaviour, it is usual to process the data by integrating over a range of angles or a range of energies to produce 1D plots. Scattered ion intensity as a function of angle yields structural information that can be used to extract parameters such as surface relaxation. Energy spectra can be used to obtain quantitative compositional information as a function of depth similar to conventional RBS but with higher resolution. With the Rutgers setup, the incident beam was normal to the surface and the TEA centre angle of 120° was chosen for several reasons. First, the 120° out direction is one of the strongest blocking directions for a (1 1 0) sample and normally incident ions. Second, it was found that the Zn and Fe surface signals were incompletely resolved for 90° scattering. A solution to improve the resolution would have been to use a higher incident energy, but the increased acquisition times necessitated by the reduced elastic scattering cross sections did not warrant such conditions. Third, it was possible for the cleaved sample to result in a macroscopically stepped surface; the influence of steps is minimized for a large angle backscattering geometry, *i.e.* the elastically scattered particles emerged at an angle 60° away from the sample normal corresponding to an outgoing blocking direction.

MEIS (*i.e.* high resolution RBS spectroscopy) utilizes elastic scattering caused by Coulomb repulsion of atomic (or ionic) cores at small interatomic distances. The electronic stopping power, dE/dx, for protons is larger in the MEIS energy region, which results in significantly improved depth resolution. A highly collimated beam of ions ($^1H^+$ or $^1H^-$ or $^4He^+$, energy of 50–200 keV) is directed at a crystalline target along a direction of high symmetry. Deflection of the incident ions from the first atom along a row parallel to the beam leads to the formation of a shadow cone, thereby reducing the probability of scattering from lattice atoms located deeper within the crystal. This channeling effect provides the surface sensitivity of the method. The majority of elastically scattered ions cannot emerge back into the vacuum if they encounter surface atoms (the so-called blocking effect) they suffer a small angle deflection. By analyzing the angular distributions of the backscattered ions, one can attempt to deduce the surface atomic geometry by comparison with Monte Carlo ion scattering simulations, generically referred to as the Vegas code [16]. Briefly, in these calculations the scattering process is simulated for specific crystal structures where surface relaxation or reconstruction, surface Debye temperature and surface adsorbates are varied until reasonable agreement with measured *absolute* blocking yields is obtained. However, since there is a vast parameter space to search, it is unlikely that reasonable fits to experimental data can be shown to be unique. To minimize surface damage by inelastically scattered ions, several spots on the sample were analysed. Each spot received an ion dose in the order of 10–15 μC.

There is a finite probability that atoms located beneath the surface will scatter incident ions on account of two factors: (i) lattice atoms are not fixed in space due to thermal vibrations and can be 'seen' by the incident beam even in a channeling configuration resulting in a non-zero hitting probability (which decreases monotonically with increasing depth into the target), and (ii) surface relaxation and/or reconstruction effects may expose subsurface atoms to the incident ion flux. The kinematics of ion scattering provide the mass (and hence chemical) specificity of the technique: *i.e.* it is possible to focus on those incident projectiles that are scattered from a particular target species by an appropriate selection of the scattered particle energy.

We emphasize here that, contrary to the situation for XPS, ion scattering studies are insensitive to the presence of chemical bonds but do measure absolute scattering yields. In principle, the information extracted from the two types of measurements are then complementary.

3. Results and discussion

3.1. EPMA

From the EPMA measurements, the high-Fe sphalerite was found to contain trace amounts of Mn (0.36 wt%) and Cd (0.62 wt%), and a total Fe concentration of 14.7 wt%. The average stoichiometry of the sample, obtained from a total of 30 spot analyses per sample, was then found to be $(Zn_{0.733}Fe_{0.254}Mn_{0.006}Cd_{0.005})S_{1.002}$, yielding an atomic ratio Zn/Fe = 2.89. Micro-XRD analysis and precession camera diffraction patterns confirmed that samples were oriented in the (1 1 0) direction.

3.2. RBS

Fig. 1 shows the RBS spectrum obtained for a scattering angle of 170°. Two samples from the same piece of sphalerite were measured and the spectra were fitted via the simulation program QUARK [24]. The stoichiometry was found to be Zn:Fe:Mn:S:Cd = 0.730(±0.04):0.263(±0.02):0.0074(±0.0005):1.00:0.0068(±0.0003) (Fe = 16.5 wt%, Zn = 49.6 wt%); the uncertainties are estimates based on the expected reliability of ^4He stopping powers [25]. In the RBS spectrum, we could not ascertain a small Mn impurity due to its small mass difference relative to Fe, but the PIXE data yield the Mn/Fe ratio, which allows the Mn concentration to be extracted directly. Thus, we obtain the atom ratio Zn/Fe = 2.78 ± 0.26. The presence of a small Cd concentration is not relevant for the present studies, and this species has been ignored in subsequent ion scattering simulations. We therefore obtain good agreement with the EPMA stoichiometric values. Deulkar et al. [26] have noted a S deficiency from EPMA measurements relative to X-ray fluorescence (XRF) results, which we do not see in these data, *i.e.* the Zn/S ratios from EPMA agree within 0.5% with those from RBS. Taguchi and Yokogawa [9] have determined a Zn:S ratio of ~0.7 from RBS measurements for an iodine-doped ZnS crystal, which may be attributable to the presence of a significant oxygen concentration as evidenced by the easily visible O signal seen in their RBS spectrum. Kashani [10] has also determined the stoichiometry

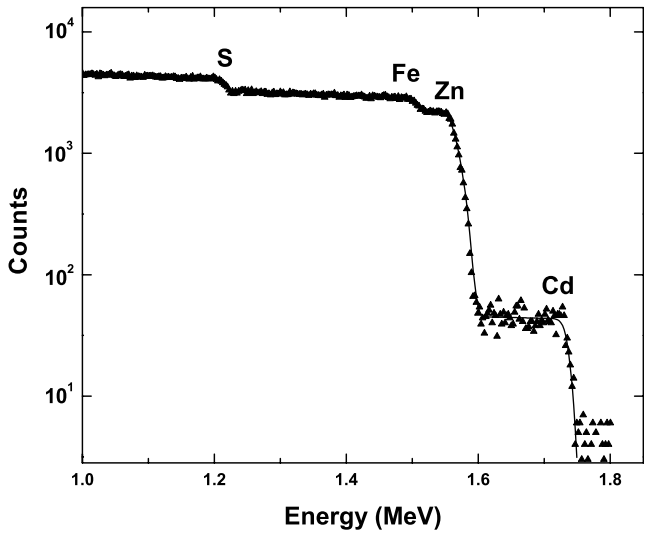

Fig. 1. Experimental Rutherford backscattering 'random' spectrum for incident 2 MeV $^4He^+$ ions recorded at 170°. The smooth curve is the result of a simulation. The edge positions for the four major target species are shown.

of ZnS thin films using RBS and finds to a first approximation that the films were stoichiometric. However, his EPMA analyses indicate significant C and O contamination: 5.3 at.% and 3.2 at.%, respectively. The presence of these low-Z impurities can certainly affect the interpretation of RBS spectrometry. We also note evidence for possible charging of his films based on the slopes of the spectral edge features of the RBS spectrum, together with his observation of blue–violet luminescence of the target upon bombardment by 25 nA of 2.3 MeV $^4He^+$ ions.

3.3. PIXE

In the PIXE technique, the $K_{\alpha,\beta}$ X-ray yields of S, Fe and Zn were measured for 18 target tilt angles with a step size of 0.3° around the ⟨1 1 0⟩ channeling direction in order to determine the position of the Fe atoms with regard to Zn atoms in the bulk. The integrated beam fluence was 3 μC for each angle. For the 'random' RBS measurements, the samples were continuously rotated around the azimuthal direction using a tilt angle of 2.5°. The Mn K_α yield was measured as well for the random data. Both RBS and PIXE results are shown in Fig. 2. The PIXE X-ray yield data show no evidence for Fe in interstitial lattice positions and suggest that Fe atoms *in the bulk* are located on Zn (or S) lattice sites, since the Fe, Zn and S yields display angular minima for the same incident alignment, *i.e.* along the ⟨1 1 0⟩ direction. Note that the depth resolution for PIXE (and RBS) measurements is poor, ~1 μm, and therefore the measurements yield only bulk stoichiometry information. In this context, it should be noted that Isaure et al. [27] have previously used the PIXE technique with a 3.07 MeV $^4He^+$ microbeam (4 μm × 4 μm beam spot) to infer the presence of sphalerite in mineral sediments from the associated Fe, Zn and S characteristic K X-ray line intensities.

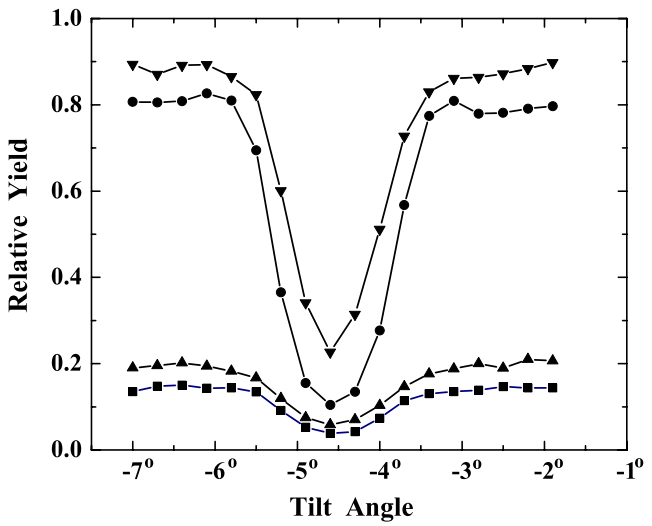

Fig. 2. Angular distribution of X-ray and RBS (energy window 0.6–0.9 MeV) yields measured in the vicinity of the ⟨1 1 0⟩ channeling direction induced by 1 MeV $^4He^+$ ions. S $K_{\alpha,\beta}$ (▼), Zn $K_{\alpha,\beta}$ (■), Fe $K_{\alpha,\beta}$ (▲) and RBS (●).

3.4. XPS

An angle-resolved XPS study of the S 2p region for the high-Fe content sphalerite was undertaken to determine the nature and position of bulk and surface contributions formed upon fracture of the mineral. Fig. 3a shows the S 2p spectra collected from an *in situ* cleaved (1 1 0) surface of sphalerite at both 90° and 20° to the detector after subtracting a Shirley-type background [28]. The spectrum collected at 90° to the sample surface enables analysis up to a depth of ~10 nm and the spectrum collected for electrons emerging at 20° to the sample surface enables analysis up to a depth of ~3 nm for photoelectron energies ~1326 eV. Previous synchrotron radiation XPS studies of transition metal sulfides [29,30] have shown that the bulk XPS S 2p signal taken at 90° contributes ~90–95% of the spectral intensity and the surface signal contributes ~5–10% of the total S intensity, independent of the packing density [28–31]. Decreasing the takeoff angle to 20° therefore provides more surface sensitivity. Calculations and

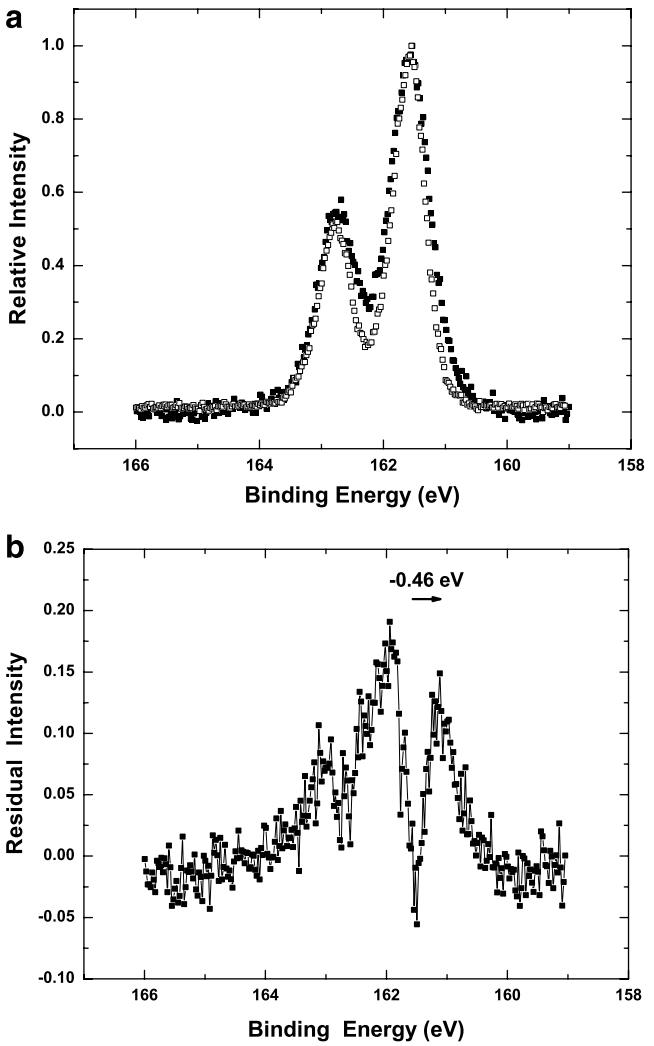

Fig. 3. (a) Angle-resolved XPS S 2p spectra of vacuum-cleaved (1 1 0) surface of sphalerite for 90° (□□□) and 20° (■■■) photoelectron takeoff angles; (b) 20–90° difference spectrum.

experiments indicate a tripling of the intensity of the surface contribution [30,32–34] for the 20° spectrum relative to the 90° spectrum. Therefore the resulting S 2p spectrum at 20° is comprised of ~15–30% surface signal. Comparison of the two spectra allows for the location and nature of surface states to be determined.

Both the 90° and 20° spectra shown in Fig. 3a exhibit two strong peaks separated by 1.19 eV with a peak area ratio of 2:1. The peaks are identified as S $2p_{3/2}$ and S $2p_{1/2}$, as predicted by spin-orbit splitting, representing bulk fully coordinated S atoms, with the $2p_{3/2}$ peak near BE ≈ 161.6 eV. Absolute binding energies cannot be obtained for insulating materials subjected to low energy electrons from a charge neutralization system. As there is no carbon or oxygen reference, the S 2p line was shifted to a binding energy close to that commonly observed for similar transition metal sulfides at BE = 161.8 eV [12]. These are the first spectra to show fully resolved $2p_{3/2}$ and $2p_{1/2}$ peaks; all other published spectra display at best a defined $2p_{1/2}$ shoulder (at higher BE) on the higher intensity S $2p_{3/2}$ peak [1,11,12,35–38]. The pronounced minima result from the excellent energy resolution obtained using the compensation system of the Kratos Axis Ultra XPS. The 20° spectrum shows significant line broadening in comparison to the more bulk-sensitive 90° spectrum.

The difference of the two spectra, where normalization has been made at the $2p_{3/2}$ peak position, is shown in Fig. 3b. This difference spectrum is comprised of three peak features representing S $2p_{3/2}$ and S $2p_{1/2}$ doublets for one surface core level shifted sulfide (S^{2-}), denoted by "A", and one surface disulfide (S_2^{2-}), denoted by "B". Here, the S $2p_{1/2}$ component of the S^{2-} doublet overlaps the S $2p_{3/2}$ component of the S_2^{2-} doublet. Considering the $2p_{3/2}$ peak for these components, the observed BE shifts are ~−0.46 eV and ~+0.3 eV for the "A" and "B" states, respectively, relative to the bulk 2p lines. Similar surface polymeric species have been identified for the *in situ* cleaved surface of other metal sulfides [31–33]. Since oxygen was not detectable at the sample surface using XPS, the oxygen concentration is less than a monolayer (<1%).

We therefore suggest that the XPS assignments show evidence for S–S bonding at the sphalerite surface. However, these data do not provide unambiguous evidence for S enrichment since the surface layer may simply reconstruct laterally to promote the formation of S–S bonds. The LEED data of Duke et al. [4] have already suggested a lateral movement of *both* S and Zn atoms for the puckered ZnS clean surface.

3.5. MEIS

The reader is referred to recent studies performed at the Daresbury MEIS facility for a generic description of the MEIS technique [39,40] as it relates to surface structure investigations. In this work, MEIS data using 130.3 keV $^4He^+$ ions incident normally along the ⟨1 1 0⟩ direction (*i.e.* for a channeling direction) are shown in Fig. 4 for both

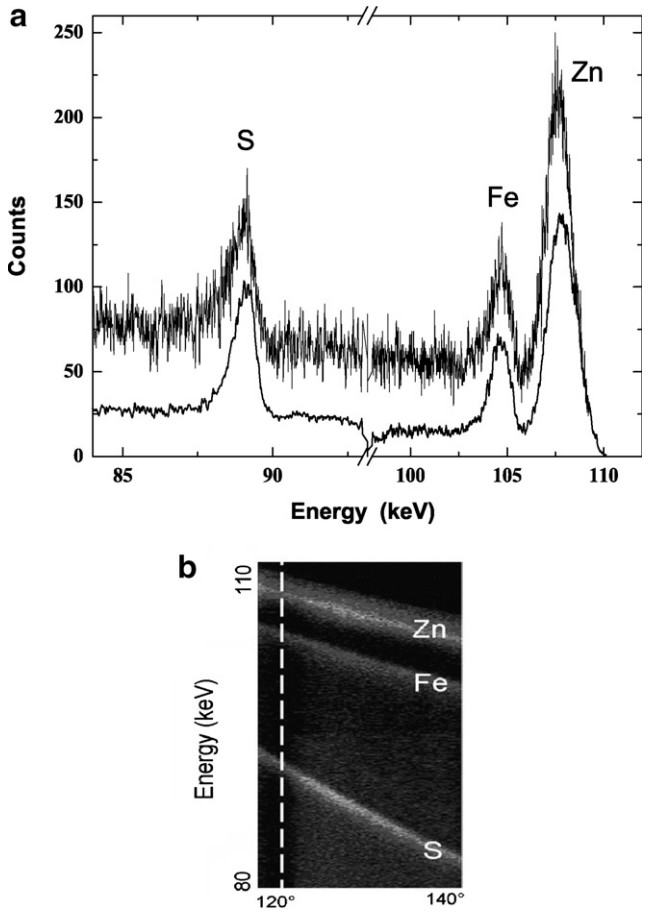

Fig. 4. Energy spectrum at a scattering angle of 120° of the air (top)- and vacuum (bottom)-cleaved samples and the MEIS 2D spectrum of the vacuum-cleaved sample measured with 130.3 keV incident $^4He^+$ ions for ⟨1 1 0⟩ *in* (*i.e.* normal incidence) and around the ⟨0 1 $\underline{1}$⟩ *out* geometry in the {$\underline{1}$ 1 2} scattering plane. The angle 120° shown by the dotted line corresponds to the blocking ⟨0 1 $\underline{1}$⟩ *out* direction. The spectra correspond to an accumulated charge equivalent to 50 μC for each TEA voltage setting (higher dose was accumulated for the vacuum-cleaved sample), and the step size was ~1 keV. The beam spot was moved frequently to avoid ion-beam damage effects and the experiment duration was ~4 h for each.

the air- and vacuum-cleaved samples. The energy (or RBS) spectra shown at the left are obtained by taking a cut through the data at an angle corresponding to the blocking minimum, *i.e.* at 120° as indicated by the dotted line shown in the 3D image at the right. The Zn and Fe signals are resolved for the entire angular range spanned by the TEA. Background subtraction was applied before extracting the angular distribution yields. The background fit was formed using a combination of linear upper and lower curves, and a polynomial curve. Fig. 5a and b shows the atomic top and side views, respectively, corresponding to the scattering geometry used here.

In order to deduce *absolute* areal densities (or visible layers) for the S, Fe and Zn species, a knowledge of the charge fraction for $^4He^+$, denoted f^+, is essential since the TEA deflects ions according to the value of E/q (E = kinetic energy, q = charge state). We have used values obtained from Marion and Young [41], which correspond to

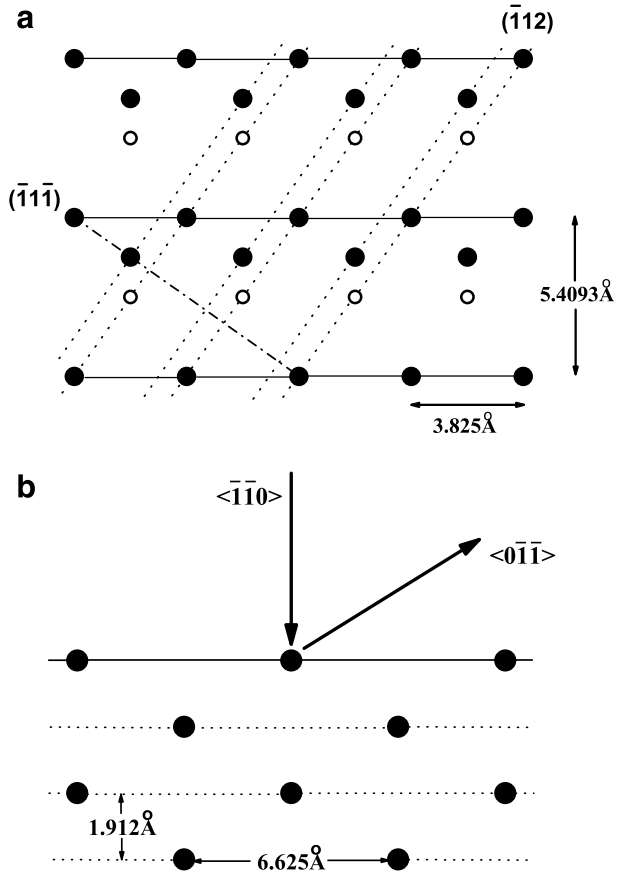

Fig. 5. (a) Top view, (1 1 0) plane. S and Zn(Fe) atom positions corresponding to different scattering planes are distinguished by white and black colour in the top view. The Zn(Fe) atom planes are shifted relative to the S atom planes by 0.781 Å. Open circles correspond to S atoms and closed circles correspond to Zn(Fe) atoms. (b) Side view, (1̄1 2) azimuth (S atoms only).

'contaminated' surfaces where f^+ is *only* a function of ion energy and is independent of the species (*i.e.* Z_2) from which the ion is scattered. We determined the normalization factors in the experiment, such as a detector solid angle and ion dose by calibration with Cu/Si and Sb/graphite standard surfaces using H^+ beam (100–130 eV incident energy range). There is evidence [42,43] that there is a marked dependence of f^+ on the scattering atom for the *first* layer of atomically clean surfaces *and* for low-Z_2: for S, this effect produces a >60% increase in f^+ at low energy [44] but vanishes for $Z_2 \geqslant 28$. Such an effect was not observed for $Z_2 = 32$ [45] or SiO_2 [44,46,47]. This topic was first investigated in the 1970s and Buck's review article [48] summarizes early results obtained for both atomically clean surfaces and 'practical' surfaces. For the sphalerite sample surfaces discussed here, even for specimens cleaved in vacuum but with no subsequent surface cleaning or preparation techniques applied (*e.g.* sputtering, annealing,...), where MEIS spectrum acquisition times were of the order of hours, where vacuum conditions were modest ($\sim 10^{-8}$ torr) during the cleaving process, for $T = 300$ K temperature conditions throughout, and where the surface has relatively high reactivity with regard to H_2O and residual hydrocarbons, we can assert with confidence that f^+ values will *not* reflect a dependence on the scattering species. An initial MEIS measurement at UWO where the sample was cleaved in an Ar-filled glovebox before insertion into the scattering chamber yielded a surface oxygen concentration of 2.5 (± 0.5) $\times 10^{15}$ atoms/cm^2, which supports this assertion. For the Rutgers experiments, oxygen was not seen in the MEIS spectra, but this observation only supports the conclusion that [O] $< 10^{15}$ atoms/cm^2. Additionally, if f^+ is markedly higher for *only* the first layer S atoms, and assuming that the surface layer contribution to the scattering yield is ~50% of the total, then one would expect to observe rather sharply peaked and distinctly asymmetric peaks in the yield as a function of energy in the region of the S peak, *i.e.* for $E \approx 88$ keV, see Fig. 4. We believe the data do not support this conclusion as the Fe, Zn and S peaks all have qualitatively the same shapes.

Let us first examine the blocking data for the air-cleaved sample, in conjunction with Vegas simulations attempting to reproduce the angular yield. Fig. 6 shows both the measured and simulated results, where the simulated curves for Fe, Zn and S correspond to the relaxed and reconstructed surface as specifically described by Duke et al. [4]. In all the simulations, it was assumed that the Zn/Fe yield was 3 in reasonable agreement with the RBS (2.78 ± 0.26) and the EPMA (2.89) values, so that the unit cell did not have to be too large in the simulations. Two sets of simulations were performed: (i) using the modified Vegas code developed at Warwick [41] for a random alloy, and (ii) using the conventional Vegas code [18] for a binary system (assuming a ZnS configuration), and then defining the Zn yield to be 75% of the output Zn yield and the Fe yield to be 25% of the output Zn yield. Both sets of simulations gave essentially identical results, as they should. Note, however, that it was necessary to increase the thermal

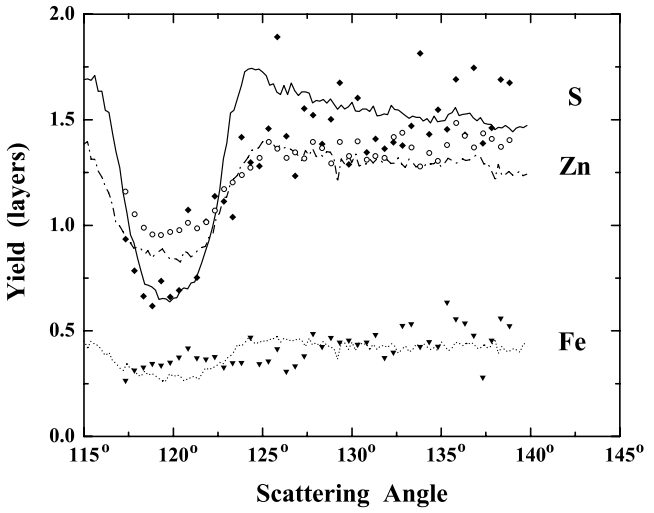

Fig. 6. MEIS experimental yields measured for the air-cleaved sample, together with simulation results. Fe ▼▼▼▼▼--------; Zn ○○○○○----------; S ♦♦♦♦♦—.

vibrations of the surface layer by 40% in order to achieve a satisfactory agreement with the experimental data. The measured Fe yield after suitable background subtraction does not show a blocking minimum. (Note that the absence of the blocking minimum in the Fe data may be due to large uncertainty in background subtraction.) So we will focus on the S and Zn measured yields. Note in Fig. 6 that the scattered ion yield measured for S is actually *lower* than that for Zn in the vicinity of the blocking minimum, *i.e.* at 120°. However, the minimum is observed at the expected angular position based on the atomic side view shown in Fig. 5b (see also 3D panel shown in Fig. 4). Since there is unlikely to be a unique surface structure that yields reasonable agreement between the data and simulation, we chose not to seek better agreement via further variations in the surface structure as the computer simulations are quite time consuming. The quality of the fit is reasonable for this structure, which is shown in a side view in Fig. 7. This model then corresponds to S atoms in the first layer that are relaxed outwards by 0.08 Å and Zn(Fe) atoms relaxed inwards by 0.51 Å, together with some translation of both species parallel to the surface. Such a relaxed and reconstructed configuration could easily produce some S–S bonding for the outermost layer. However, the XPS data taken in UHV at $T = 200$ K cannot be directly compared to the sample conditions present for the MEIS experiments.

For the vacuum-cleaved sample, the MEIS angular distribution spectrum is shown in Fig. 8. There is a marked difference compared to the air-cleaved sample: specifically, the S and Zn yields do *not* cross in the vicinity of the blocking minimum. The simulation presented here corresponds to a bulk-terminated surface. However, the measured S yield is somewhat too large relative to the simulation. Fig. 9 shows the results for a bulk-terminated surface where the S atoms have been displaced laterally by 0.5 Å. The simulated S yield increases by ~25% while the Zn and Fe simulated yields remain largely unchanged for this so-called 2-layer incidence geometry. The simulation results would be the same for S displacements in both X and Y directions (where Z is directed into the sample) and virtually independent of the displacement magnitude (except that if the S atom displacement positions the S

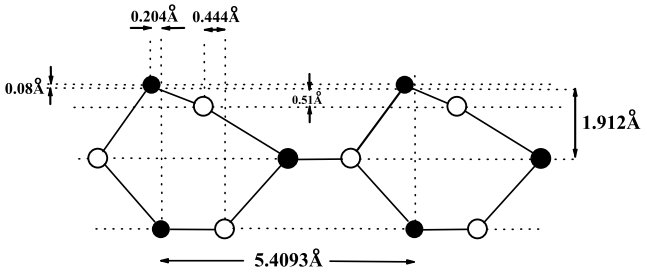

Fig. 7. side view of the (1 1 0) sphalerite surface showing the structure that results in a reasonable fit of the simulation to the air-cleaved MEIS blocking data shown in Fig. 6. Open circles correspond to S atoms and closed circles correspond to Zn (or Fe) atoms.

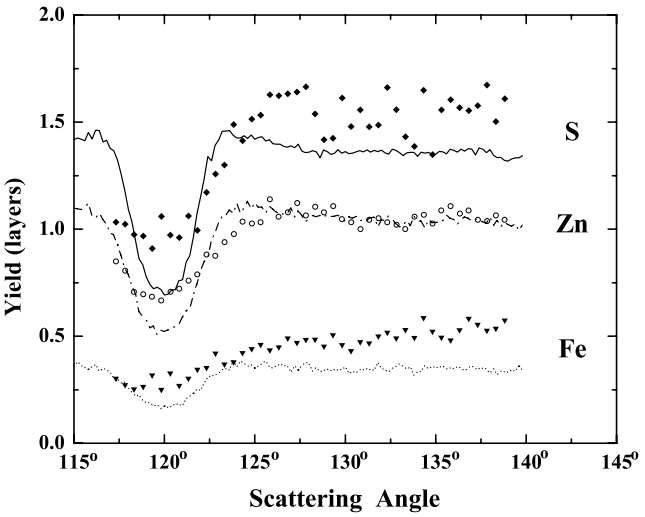

Fig. 8. MEIS experimental yields measured for the vacuum-cleaved sample, together with simulation results for a bulk-terminated surface. Symbols are the same as in Fig. 6.

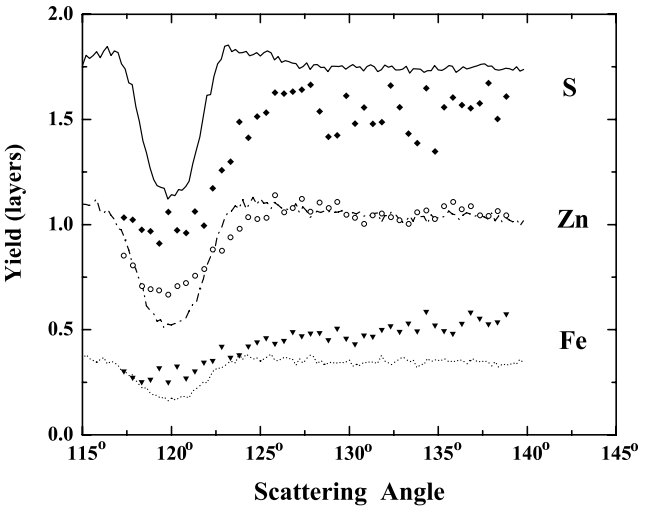

Fig. 9. MEIS experimental yields measured for the vacuum-cleaved sample, together with simulation results for a bulk-terminated surface but with surface S atoms translated laterally by 0.5 Å (in either X or Y direction). Symbols are the same as in Fig. 6.

atoms in the Zn scattering plane, then the calculated Zn yield is decreased by ~5% due to the S atoms shadowing the Zn atoms with respect to the incoming beam direction – a decrease that is too small to be measurable). In this case, the measured S yield is too low.

Both the S and Zn blocking minima appear wider and shallower in the experimental data, which can be caused by a disordered contamination layer and its effect on emerging particles. Alternatively, this modification to the blocking dip would also be observed if the S atoms were displaced in a semi-random manner. So there are two possibilities: a bulk-terminated surface with some excess S atoms located out of registry, or some disorder in the bulk-terminated surface with no excess S. We cannot

differentiate between these two possibilities with the experimental data, as both surface structures produce a simulated S yield that is larger than for a purely bulk-terminated surface, but smaller than for the case that all the S atoms are translated laterally (X or Y) off the bulk lattice sites. The results are then suggestive of some S–S bonding in the surface layer due to the enhanced yield for S. However, we are reminded again that MEIS yields are not sensitive to the presence (or type) of chemical bonds. As well, the incident ions are channeled with respect to atoms *in the bulk*, and the surface layers may be somewhat disordered leading to an increased scattered intensity. Some surface contamination may also be the source of such disorder. If an adsorbate bonds to the atoms in the surface to change the structure in some 'random' manner, *i.e. not* following a periodic pattern, then the incident ion beam would 'see' a mixture of ordered surface and 'random' surface. The yield will increase and the blocking dips will become wider and shallower – in effect washing out the blocking structure. For example, some recent MEIS studies have focused on a heavily oxidized surface [49].

There is a slope to the Fe experimental data that is difficult to understand: if it is an artifact caused by the detector response, then such an effect should be present for both S and Zn as well. We can suggest that the relatively larger uncertainty due to background subtraction under the Fe peak (see Fig. 4, $E \approx 105$ keV) is responsible for this systematic effect.

In summary, the surface condition for this vacuum-cleaved specimen should describe a situation similar to that for the XPS data (albeit with a different temperature) where S–S bonding has been shown to exist. Thus, both possibilities for the derived surface structure extracted from Vegas fits to the vacuum-cleaved MEIS spectrum are consistent with the XPS measurements.

4. Conclusions

We have studied the composition and structure of a high-Fe sphalerite (1 1 0) single crystal using a variety of analytical methods. The bulk composition as determined from RBS and EPMA analyses yielded results that were consistent with expectations, *i.e.* the sample was $Zn_{1-x}Fe_xS$, where $x \approx 0.25$. As well, the Fe atoms in the bulk were found to occupy Zn lattice positions based on the PIXE ion beam measurements using the channeling technique.

High resolution XPS spectra taken at both 90° and 20° takeoff angles for a sample that was cleaved in UHV and held at $T < 200$ K showed evidence for S–S bonding, based on the BE values in comparison to earlier studies. Not surprisingly, there was no evidence for elemental S, which may have been expected to volatilize in the UHV in any case. As well, the intensity of S 2p transitions corresponding to threefold coordinated S was small but measurable for the 20° surface sensitive spectrum, and barely evident for the 90° spectrum. No quantitative conclusions concerning excess S segregation at the surface could be drawn from the XPS data.

The MEIS data show distinctly different blocking results for the (1 1 0) sphalerite samples cleaved in vacuum and in air. The data have been successfully reproduced by Monte Carlo simulations employing different surface structures. For all the simulations, we have used a Zn/Fe ratio of 3.0 although the stoichiometry measurements indicate a slightly smaller value, ~2.8. The effect of this approximation is expected to be negligible. The surface structures arising from the different cleaving conditions are thus shown to be non-equivalent. However, for both cases, we have reproduced the MEIS data using surface structures where the S atoms are not on lattice sites, thereby conferring the possibility of S–S (*i.e.* dimer) bonding. It has not been possible to determine specific S atom locations using a single ion beam incident geometry. A full surface structure determination, to confirm the presence of dimers for example, would require having MEIS blocking data corresponding to many different scattering geometries and complementary comparisons to several simulation models. As well, MEIS analyses have normally been applied to atomically clean surfaces – conditions which are experimentally challenging to maintain for sphalerite, *i.e.* there are too many uncontrolled experimental parameters for this system (temperature, surface contamination,...). We then suggest that temperature-induced and adsorbate-induced reconstructions of the surface atomic geometry for sphalerite should be examined separately. A further question relates to reactivity as a function of Fe loading, which would materially affect contaminants and thereby alter the surface chemistry.

Acknowledgements

We would like to acknowledge Mr. J. Hendriks for his assistance with the MEIS experiments at UWO, Prof. T. Gustafsson for providing generous access to the Rutgers MEIS facility and Prof. G.M. Bancroft (Chemistry, UWO) for his many insightful suggestions. This project received funding assistance from the Center for Chemical Physics (CCP) at UWO and from the Natural Sciences and Engineering Research Council (NSERC-Canada).

References

[1] C.G. Weisener, R.St.C. Smart, A.R. Gerson, Int. J. Miner. Process. 74 (2004) 241.
[2] D.J. Vaughan, U. Becker, K. Wright, Int. J. Miner. Process. 51 (1997) 1.
[3] A.B. Kashyout, A.S. Aricò, N. Giordano, V. Antonucci, Mater. Chem. Phys. 41 (1995) 55.
[4] C.B. Duke, R.J. Meyer, A. Paton, A. Kahn, J. Carelli, J.L. Leh, J. Vac. Sci. Technol. 18 (1981) 866.
[5] C.B. Duke, A. Paton, A. Kahn, J. Vac. Sci. Technol., A 2 (1984) 515.
[6] Y.R. Wang, C.B. Duke, Phys. Rev. B 36 (1987) 2763.
[7] C.B. Duke, Y.R. Wang, J. Vac. Sci. Technol., B 6 (1988) 1440.
[8] H.M. Steele, K. Wright, I.H. Hillier, Phys. Chem. Miner. 30 (2003) 69.

[9] T. Taguchi, T. Yokogawa, J. Phys. D: Appl. Phys. 17 (1984) 1067.
[10] H. Kashani, Thin Solid Films 288 (1996) 50.
[11] R.St.C. Smart, W.M. Skinner, A.R. Gerson, Surf. Interface Anal. 28 (1999) 101.
[12] C.G. Weisener, R.St.C. Smart, A.R. Gerson, Geochim. Cosmochim. Acta 67 (2003) 823.
[13] A. Boulton, D. Fornasiero, J. Ralston, Int. J. Miner. Process. 70 (2003) 205.
[14] R.G. Smeenk, R.M. Tromp, H.H. Kersten, A.J.H. Boerboom, F.W. Saris, Nucl. Instrum. Methods Phys. Res. 195 (1982) 581.
[15] R.M. Tromp, J. Vac. Sci. Technol., A 1 (1983) 1047.
[16] R.M. Tromp, J.F. van der Veen, Surf. Sci. 133 (1983) 159.
[17] R.M. Tromp, H.H. Kersten, E. Granneman, F.W. Saris, R. Koudijs, W.J. Kilsdonk, Nucl. Instrum. Methods Phys. Res., Sec. B 4 (1984) 155.
[18] J.F. van der Veen, Surf. Sci. Rep. 5 (1985) 199.
[19] L. Smit, J.F. van der Veen, Surf. Sci. 166 (1986) 183.
[20] R.M. Tromp, M. Copel, M.C. Reuter, M. Horn von Hoegen, J. Speidell, R. Koudijs, Rev. Sci. Instrum. 62 (1991) 2679.
[21] K. Wright, G.W. Watson, S.C. Parker, D.J. Vaughan, Am. Mineral. 83 (1998) 141.
[22] I. Kartio, K. Laajelehto, E. Suoninen, S. Karthe, R. Szargan, Surf. Interface Anal. 18 (1992) 807.
[23] V.P. Zakaznova-Herzog, S.L. Harmer, H.W. Nesbitt, G.M. Bancroft, R. Flemming, A.R. Pratt, Surf. Sci. 600 (2006) 348.
[24] W.N. Lennard, website: see <http://www.uwo.ca/isw/~wlennard>.
[25] J.R. Tesmer, M. Nastasi, Handbook of Modern Ion Beam Materials Analysis, Materials Research Society, Pittsburgh, PA, 1995 (Chapter 4).
[26] S.H. Deulkar, C.H. Bhosale, M. Sharon, Mater. Chem. Phys. 89 (2005) 211.
[27] M.-P. Isaure, A. Laboudigue, A. Manceau, G. Sarret, C. Tiffreau, P. Trocellier, G. Lamble, J.-L. Hazemann, D. Chateigner, Geochim. Cosmochim. Acta 66 (2002) 1549.
[28] L. Ley, R.A. Pollak, F.R. McFeely, S.P. Kowalzcyk, D.A. Shirley, Phys. Rev. B 9 (1973) 600.
[29] M.P. Seah, W.A. Dench, Surf. Interface Anal. 1 (1979) 2.
[30] S.L. Harmer, H.W. Nesbitt, Surf. Sci. 564 (2004) 38.
[31] D. Briggs, M.P. Seah, Practical Surface Analysis 1, John Wiley and Sons, 1990.
[32] S.L. Harmer, A.R. Pratt, H.W. Nesbitt, M.E. Fleet, Am. Mineral. 89 (2004) 1026.
[33] S.L. Harmer, A.R. Pratt, H.W. Nesbitt, M.E. Fleet, Can. Mineral. 43 (2005) 1619.
[34] J. Mycroft, A.R. Pratt, H.W. Nesbitt, Geochim. Cosmochim. Acta 59 (1995) 721.
[35] E. Godoćíková, P. Baláz, Z. Bastl, L. Brabec, Appl. Surf. Sci. 200 (2002) 36.
[36] T. Ben Nasrallah, M. Amlouk, J.C. Bernede, W. Belgacem, Phys. Status Solidi A 201 (2004) 3070.
[37] A.N. Buckley, H.J. Woutherlood, R. Woods, Hydrometallurgy 22 (1989) 39.
[38] A.N. Buckley, R. Woods, H.J. Wouterlood, Int. J. Miner. Process. 26 (1989) 29.
[39] D. Brown, P.D. Quinn, D.P. Woodruff, T.C.Q. Noakes, P. Bailey, Surf. Sci. 497 (2002) 1.
[40] C.J. Baddeley, L.H. Bloxham, S.C. Laroze, R. Raval, T.C.Q. Noakes, P. Bailey, J. Phys. Chem. B 105 (2004) 2766.
[41] J.B. Marion, F.C. Young, Nuclear Reaction Analysis: Graphs and Tables, North-Holland, 1968, p. 37.
[42] R.S. Bhattacharya, W. Eckstein, H. Verbeek, Surf. Sci. 93 (1980) 563.
[43] K. Kimura, H. Ohtsuka, M. Mannami, Phys. Rev. Lett. 68 (1992) 3797.
[44] Y. Hoshino, S. Semba, T. Okazawa, Y. Kido, Surf. Sci. 515 (2002) 305.
[45] K. Nakajima, A. Konishi, K. Kimura, Phys. Rev. Lett. 452 (1999) 1802.
[46] K. Kimura, K. Nakajima, Y. Okazaki, Nucl. Instrum. Methods Phys. Res., Sec. B 183 (2001) 166.
[47] K. Nakajima, Y. Okura, M. Suzuki, K. Kimura, Nucl. Instrum. Methods Phys. Res., Sect. B 219–220 (2004) 514.
[48] T. Buck, in: N.H. Tolk, J.C. Tully, W. Heiland, C.W. White (Eds.), Inelastic Ion-Surface Collisions, Academic Press, 1977, p. 47.
[49] M.A. Muñoz-Márquez, R.E. Tanner, D.P. Woodruff, Surf. Sci. 565 (2004) 1.